The Outer Lindblad Resonance and the Morphology of Early Type Disk Galaxies

R. Buta – University of Alabama
D. A. Crocker – University of Alabama

Citation of published version:

Buta, R., Crocker, D., (1991): The Outer Lindblad Resonance and the Morphology of Early Type Disk Galaxies. *The Astronomical Journal*, 102(1). DOI: 10.1086/115991

THE ASTRONOMICAL JOURNAL VOLUME 102, NUMBER 5 NOVEMBER 1991

THE OUTER LINDBLAD RESONANCE AND THE MORPHOLOGY OF EARLY TYPE DISK GALAXIES

R. BUTA[1] AND D. A. CROCKER[1]
Department of Physics and Astronomy, University of Alabama, Tuscaloosa, Alabama 35487
Received 17 May 1991; revised 3 July 1991

ABSTRACT

The morphology of outer rings and pseudorings in SB and SAB galaxies includes a number of distinct categories that bear a remarkable resemblance to the gaseous rings which have developed near the outer Lindblad resonance in *n*-body models of barred spirals. This paper displays these categories using CCD images and color index maps of 22 galaxies from the Catalogue of Southern Ringed Galaxies (CSRG). The prominence of the OLR morphologies in these and many other galaxies provides an important handle on pattern speeds of bars and ovals, as well as insights into internal dynamics. It also provides an important distinction to be considered when comparing early and late-type galaxies. An interesting possible correlation between the presence of nuclear star formation and outer ring/pseudoring morphology emerges from the new images. In a class of rings where the arms wind $\sim 180°$ with respect to the ends of a bar or oval, 9 out of 11 of our examples display blue nuclei or circumnuclear rings in a $B-I$ color index map. This contrasts with a class where the arms wind $\sim 270°$ with respect to the ends of a bar or oval, for which only 3 out of 11 of our examples display nuclear star formation. We also find a similar correlation regarding the presence or absence of a clear dust lane pattern within the region of a bar or inner oval. The reasons for these correlations are not obvious, and a larger sample is needed to verify them. An interesting finding is that the triple-ringed S0/a galaxy NGC 1326 contains a remarkable pattern of dust lanes in the region of its weak bar that bears no resemblance to any model. We also present images of eight additional CSRG galaxies which display morphological details of special interest. For example, ESO 566 – 24 is an exceptionally regular four-armed ringed barred spiral that is rare in the CSRG, while ESO 565 – 11 is an unusual object with a large nuclear ring of blue knots, a peculiar bar, and atypical inner and outer pseudorings. Other cases are described in an Appendix.

1. INTRODUCTION

One of the goals of extragalactic studies has always been to understand the dynamics underlying the morphology of galaxies. This has never been an easy task, and it has been complicated in recent years by the realization that the visible components of galaxies may comprise only a small fraction of their total mass. However, the experience of the last decade or so has demonstrated the value of highly focused research on one galaxy type or a small range of types. Progress in understanding E's and S0's, for example, has clearly benefitted from the concerted effort world wide of a large number of astronomers. This approach has also been fruitful for barred galaxies, irregular galaxies, and interacting galaxies.

Ringed galaxies are especially worthy of such a focused approach. Rings and pseudorings are so abundant among normal, massive early type disk galaxies that only natural processes of galactic evolution could be involved in their development. Such processes almost certainly include gravity torques, dissipation, and self-gravity. Rings do not point *directly* to those effects, but because of their suspected association with orbital resonances, rings are visible probes of internal dynamics. If we can associate certain rings with specific resonances uniquely, then the location of a ring will provide an indirect way of measuring the pattern speed of an internal nonaxisymmetric perturbation when kinematic information is available. Since little is known about pattern speeds, which are fundamental in all theoretical models of spiral or barred disk galaxies, rings may provide one of the most reliable ways of determining this parameter.

The commonly observed and distinctive outer rings and pseudorings of SB and SAB galaxies are prime candidates for an association with the *outer Lindblad resonance*, or OLR, which is just one of the major low-order resonances that could be important in a disk system. This association was suggested by Schwarz (1981) on the basis of *n*-body models, and it would be a major advance in our understanding of barred systems if we could prove, even indirectly, that such an association is correct. In fact, several lines of evidence are now known which strongly support the suggestion, one of which is *morphology*[2]: it was shown by Buta (1986, hereafter referred to as B86) that the two types of OLR pseudorings discovered by Schwarz can be identified in many galaxies. However, the images presented in B86 were based on PDS scans of SRC-J copy films and were only barely adequate for illustrating the types. In this paper we present images of many of the same galaxies as in B86, but based on CCD observations with the CTIO 1.5 m telescope. These represent a considerable improvement over the images in B86. With the new images we try to establish the different subclasses of outer rings and pseudorings (see Fig. 1) more clearly and definitively than before, and how they are related to the model OLR rings discovered by Schwarz. In addition, we provide more accurate information on the inner regions of the galaxies as well as color index maps to examine possible correlations of bar and nuclear structures with the outer ring/pseudoring morphologies. As in B86, the sample was chosen from the Catalogue of Southern Ringed Galaxies, or CSRG, being prepared from the SRC IIIa-J southern sky survey [see Buta (1991a) for a summary of the status of the work]. The observations and sample are presented in Sec. 2. A sum-

[1] Visiting Astronomer, Cerro Tololo Inter-American Observatory, National Optical Astronomy Observatories, which is operated by the Association of Universities for Research in Astronomy, Inc. (AURA), under cooperative agreement with the National Science Foundation.

[2] The others are ring ratios (Athanassoula *et al.* 1982) and apparent bar/ring alignments (see Buta 1986, and references therein).

 0004-6256/91/051715-09$00.90

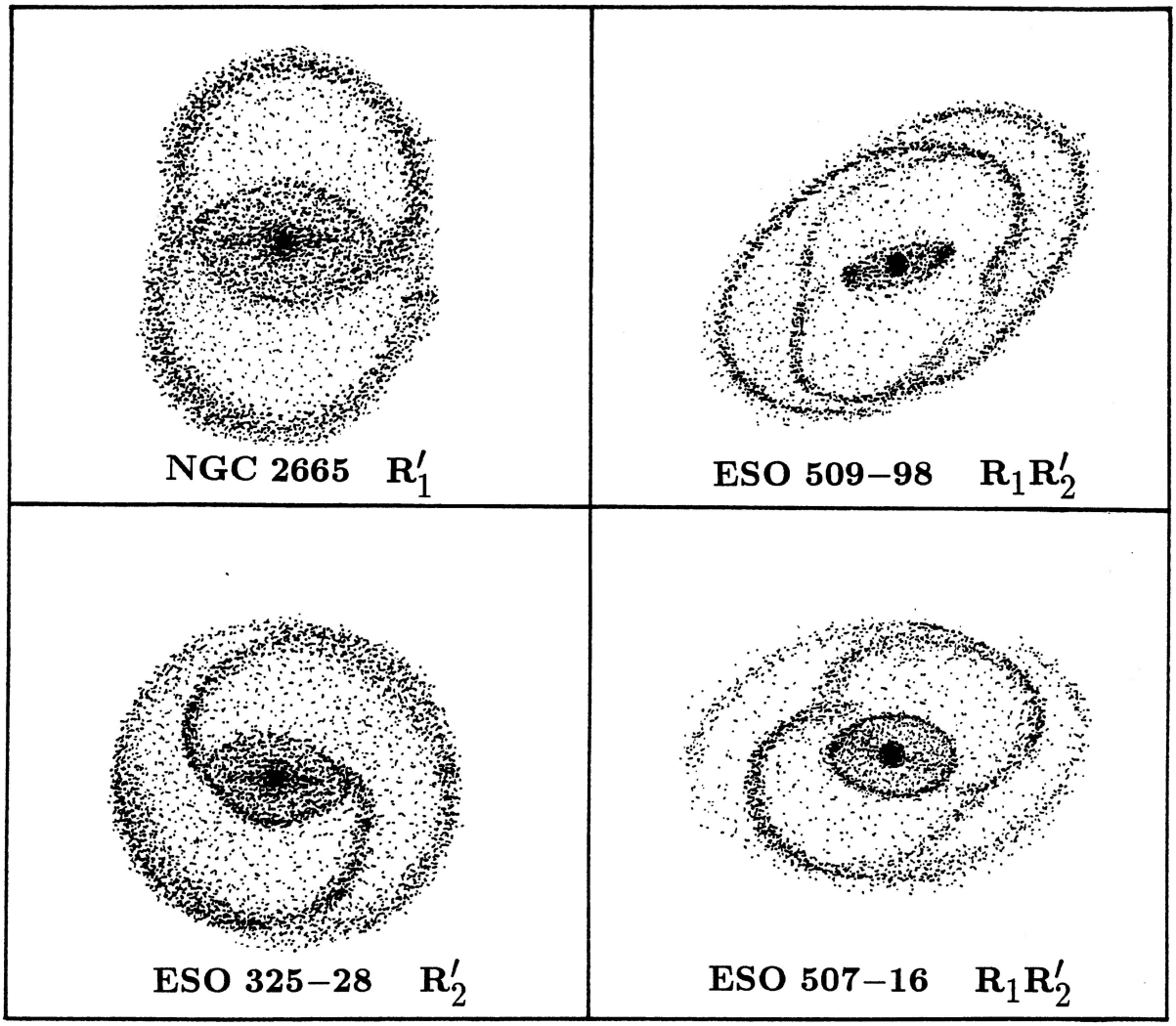

FIG. 1. Schematics of prototypes of the main classes of suspected OLR pseudorings.

mary of the morphological subclasses of outer pseudorings is given in Sec. 3, and a discussion is given in Sec. 4. Conclusions and prospects for future work are provided in Sec. 5. A few special cases from the CSRG are discussed in an appendix.

2. OBSERVATIONS

A total of 30 outer-ringed and pseudoringed galaxies was observed in 1990 February using the TI #3 CCD on the 1.5 m telescope of Cerro Tololo Inter-American Observatory. All but one are from the CSRG. These were also measured photometrically with standard *UBVRI* filters in a range of aperture sizes with a GaAs photometer and the ASCAP program on the CTIO 1.0 m telescope (Buta & Crocker 1991). The CCD observations were mostly made in the *B*, *V*, and Cousins *I* passbands in order to obtain color information, which is presented here only in the form of color index maps. Each image was bias corrected and flatfielded and, for the *I* band only, fringe-frame corrected, using standard IRAF[3] routines. The final images for display were sky subtracted and normalized to the sky level, then converted to units of mag arcsec^{-2} using zero points derived from the aperture photometry. For the purposes of the photographs we have ignored small color terms in the transformation from the CCD natural system to the Johnson and Cousins standard systems, but these terms will be taken into account in the analysis of the surface photometry to be given in a later paper.

The selected sample of ringed galaxies is summarized in Table 1. Column (1) gives the 1950 coordinates taken from either Lauberts (1982) or the RC2 (de Vaucouleurs *et al.* 1976). Column (2) gives the catalog name [usually from the same sources as column (1)]. Column (3) gives the major

[3] IRAF is distributed by National Optical Astronomy Observatories, which is operated by the Association of Universities for Research in Astronomy, Inc., under cooperative agreement with the National Science Foundation.

TABLE 1. Classifications based on CCD frames.

α (1950) δ 1	Name 2	D 3	Ring 4	CSRG Type 5	H Type 6	Bar 7	Dust 8	Center 9
0322.0 −3638	NGC 1326	2.'74	R_1	(R_1)SAB(r,nr)0/a	RSB0_3/SBa(r)	ans/reg:	pec	blue nr
0345.2 −3352	IC 1993	1.51	R′	(R′)SA(s)bc	Sbc(s)	....	....	red nuc
0431.3 −3326	ESO 360− 15	0.78	R_1'	(R_1')SB(rs)a	SBa(rs)	ans	....	blue nuc
0621.9 −3211	ESO 426− 2	1.07	R_1	$(\underline{R}_1R_2')$SB(r)0/a	SBa(r)	reg	....	red nuc
0635.0 −3502	ESO 365− 35	1.05	R_2'	(R_2')S$\underline{\text{A}}$B(l)0/a	Sa(s)	reg	....	red nuc
0843.8 −1907	NGC 2665	1.85	R_1'	(R_1')SA$\underline{\text{B}}$(rs)a	Sa/SBa(s)	reg/oval	c?	blue nuc
0934.4 −2054	NGC 2935	2.80	R_2'	(R_2')SA$\underline{\text{B}}$(l,nr)b pec	Sb/SBb(s)	reg	a	blue nr
0941.4 −2015	NGC 2983	1.62	L	(L)SB(s)0^+	SB0_2/SBa(s)	ans	....	red nuc
0951.2 −1921	ESO 566− 24	1.17	R′	(R′)SB(r)b	SBb(r)	ans/reg	a	blue nuc/nr
0927.0 −2010	ESO 565− 11	1.30	$\underline{\text{r}}$s	(R′:)SB($\underline{\text{r}}$s,nr)a pec	SBa(s) pec	pec	c?	blue nr
1027.7 −3458	NGC 3269	1.68	R_2'	(R_2')SAB(rl)a	Sa(s)	reg?	....	red nuc
1035.1 −2603	ESO 501− 51	2.08	R′	(R′)SA(rs)ab	Sab(s)	....	....	red nuc
1037.6 −2956	ESO 437− 33	1.12	R_1'	(R_1')SAB(rl)a	Sa/SBa(s)	comp/oval	c?	blue nr
1041.3 −3609	NGC 3358	2.91	R_2'	(R_2')SAB(l)ab	Sab/SBab(s)	ans	....	red nuc + nb
1049.9 −3224	ESO 437− 67	2.46	R_1'	(R_1')SB($\underline{\text{r}}$s,nr)a$\underline{\text{b}}$	SBb(rs)	reg	b	blue nr
1050.4 −4454	ESO 264− 47	1.06	R_2'	(R_2')S$\underline{\text{A}}$B($\underline{\text{r}}$l)a	Sa(r)	ans/oval	....	red nuc
1056.3 −4619	NGC 3482	1.51	R_1	(R_1R_2')SAB($\underline{\text{r}}$s)a	RSa/SBa(rs)	ans/reg	....	red nuc
1100.5 +2815	NGC 3504	2.05	R_1'	(R_1')SA$\underline{\text{B}}$($\underline{\text{r}}$s)ab	Sb/SBb(s)	reg	c	part blue nr
1233.4 −3910	NGC 4553	1.80	RL	(RL)SA(r)0^+	S0_3/Sa(r)	....	....	red nuc + nb
1247.0 −2453	ESO 507− 16	0.90	R_1	$(\underline{R}_1R_2')$S$\underline{\text{A}}$B($\underline{\text{r}}$l)a	Sa(r)	arch ans?	....	blue nr
1258.5 −1756	ESO 575− 47	1.63	R_1'	(R_1')SB($\underline{\text{r}}$s)ab	SBb(sr)	reg	....	red nuc
1259.2 −4230	NGC 4909	1.52	R_2'	(R_2')SA(l)$\underline{\text{a}}$b	Sa(s)	oval	....	red nuc
1314.9 −3150	IC 4214	1.93	R_1	(R_1)SA($\underline{\text{r}}$s,nr)a	Sa(rs)	oval	comp	blue nr +spir
1322.6 −2052	NGC 5134	3.36	R_1	(R_1)SA$\underline{\text{B}}$($\underline{\text{r}}$l,nl)ab	RSb/SBb	reg	comp	red nuc
1322.9 −2612	ESO 508− 78	0.90	R_1'	(R_1')SB($\underline{\text{r}}$s)a	SBa(s)	reg	....	blue nuc
1328.7 −2100	ESO 577− 3	0.90	R_2'	(R_2')SB(r)ab	SBa(r)	reg	....	red nuc
1332.5 −2746	IC 4290	2.13	R_1'	(R_1')SB(r)a	SBa(r)	reg	....	red nuc
1340.6 −2541	ESO 509− 98	1.07	R_2'	(R_1R_2')SB(s)a	SBa(s)	ans	....	red nuc
1347.7 −3812	ESO 325− 28	1.06	R_2'	(R_2')SB(r)b	SBb(r)	reg	....	blue nuc
1439.6 −1702	NGC 5728	3.69	R_1	(R_1)SA$\underline{\text{B}}$(r,nr)a	RSBab(rs)	reg	a	blue nr

Explanations:

Col. 1. Right ascension and declination from Lauberts (1982) or RC2.

Col. 2. Catalog name.

Col. 3. Diameter of primary ring or pseudoring feature.

Col. 4. Identity of primary ring or pseudoring feature.

Col. 5. Classification (by R. Buta) in the CSRG system, which is a modified de Vaucouleurs' (1959) revised Hubble system that recognizes subclasses of outer rings and lenses (see text).

Col. 6. Classification (by R. Buta) using Sandage and Tammann (1987) revised Hubble system.

Col. 7. Bar type: reg = regular SB-type bar; ans = "ansae"-type bar; arch ans = ansae bar where blobs are bright arches in an inner ring; comp = complex bar; oval = oval distortion; pec = peculiar bar.

Col. 8. Dust lane type in bar or oval region: a, b, and c refer to typical bar dust lane types illustrated by Athanassoula (1984; see text); comp = complex and asymmetric; pec = peculiar not because of irregularity or asymmetry.

Col. 9. Characteristics of center: red nuc = red nucleus; blue nuc = blue nucleus; blue nr = blue circumnuclear ring; nb = nuclear bar.

axis diameter of the ring feature identified in Column (4) in arcminutes, usually obtained with a 7× Bausch and Lomb measuring magnifier used with the sky surveys. These sizes can be used as an indication of the scale of the images. Column (5) gives estimates (by R.B.) of the Hubble type in a modified de Vaucouleurs' system taking into account refined ring classifications (see below) and also including the explicit recognition of lenses as proposed by Kormendy (1979). These types are based on the blue light images only since the system is defined in the *B* band. Column (6) gives types estimated (also by R.B. and from the *B* images) in the revised Hubble system presented by Sandage (1961) and Sandage & Tammann (1987, hereafter referred to as RSA); these are considerably simpler than the column (5) types, but in general do not recognize most of the ring features of interest. Column (7) provides a rough bar classification (see Sec. *4.2*), while column (8) provides a classification of the dust lane pattern in the bar or oval region if such a pattern is present, based on inspection of the color index maps (see Sec. *4.3*). Finally, column (9) provides information on nuclear structure which, except for two nuclear bars, is also based on inspection of the color index maps (see Sec. *4.4*).

The objects in Table 1 represent only a small fraction of the galaxies in the CSRG where the outer ring or pseudoring can be subclassified into the B86 categories. There are nearly 300 cases in the current version of the CSRG (see Buta 1991a), and many more have been found north of the CSRG's $-17°$ declination limit on the charts of the Palomar Sky Survey. A more extensive list of these objects, prepared by Buta, can be found in an appendix to the introduction to the *Third Reference Catalogue of Bright Galaxies* (de Vaucouleurs *et al.* 1991). Many of the Table 1 galaxies are also in that list, but in a few cases the types are slightly different, due to a re-evaluation.

The atlas of images and color index maps is presented in Figs. 2–13 [Plates 45–56]. For most of the galaxies, the blue light image is displayed on the left. The images of ESO 508 − 78 and ESO 507 − 16 are *V* band, and that of ESO 360 − 15 is a hybrid $B + V$ image, to provide a somewhat better signal-to-noise ratio. To the right of each galaxy image is its color index map, usually $B - I$, except for NGC 2983 and ESO 575 − 47 where the map is $B - V$. (The $B - V$ image of ESO 575 − 47 is seriously affected by scattered light from a bright red star.) The range of colors displayed is usually 1.25–2.75 or 1.50–2.50 for $B - I$ and 0.25 to 1.25 for $B - V$, and the gray scale is such that dark features are blue and red features are light. These maps provide the most extensive display of the distribution of star formation ever presented for ringed galaxies.

3. THE CSRG AND THE SCHWARZ OLR RING TYPES

The focus of this paper is on normal galaxies having outer pseudorings classified as being of types R_1' and R_2', or the combined type R_1R_2' in the CSRG. These are the features suspected to be related to the gaseous rings which developed near the OLR in Schwarz's simulations. A description of the types was given by Buta (1986, 1989). The key to searching effectively for these morphologies has been the high quality of the SRC-J southern sky survey, whose resolution and limiting surface brightness of ~ 27 mag arsec^{-2} allow the easy detection of the characteristically faint outer rings and pseudorings. These features tend to have peak surface brightnesses of only 10%–20% of the night sky or less ($\mu_B \gtrsim 24$–25 mag arcsec^{-2}) in blue light. Although the morphologies of several outer ringed and pseudoringed galaxies are well illustrated in a few excellent atlases (e.g., Sandage 1961; Sandage & Tammann 1987; Sandage & Bedke 1988), the SRC charts allow recognition and study of vastly superior numbers in a wider range of orientations and environments. One of the main goals of the CSRG has been to catalog these galaxies in a homogeneous way to provide samples for serious statistics and for detailed follow-up studies.

Figure 1 presents an improved schematic (compared to those in Buta 1986, 1989) of the suspected OLR ring types based on four excellent prototypes from the CCD sample. These drawings are designed to present the structures of interest without being confused by detail; they were traced directly from the CCD photographs and are based on NGC 2665 (R_1'; see Fig. 2), ESO 325 − 28 (R_2'; see Fig. 5), ESO 509 − 98 (R_1R_2'; see Fig. 8), and ESO 507 − 16 (R_1R_2'; see Fig. 8). In the following sections we discuss the characteristics that define these subclasses and how they relate to the Schwarz models.

3.1 The R_1' and R_2' Morphologies

The distinguishing characteristic of the R_1' morphology is a winding of the arms of about 180° with respect to the ends of a bar or oval, such that the arms intersect each other near the axis of this feature. The arms can either break directly from the ends of the bar or oval, as in NGC 2665, or from a point on an inner ring or lens near the minor axis line of the bar or oval. That is, the total winding of the arms can exceed 180°. Figures 2 and 3 illustrate six examples of R_1' pseudorings, all of which are representative. In at least five of these objects, the elongation of the R_1' is nearly perpendicular to the bar or oval, though none were chosen for this reason. Related cases (see next section) are shown in Figs. 4 and 9, and a few other possibly related cases are shown in Figs. 10 and 12.

On the basis of the Schwarz models, the R_1' type of pseudoring could be interpreted in one of two ways. The first is that the type is related to the family of periodic orbits which lie just *inside* the OLR and which are aligned perpendicular to the bar (see Figs. 4 and 12 of Schwarz 1981). This type was favored by weak bars and an initial gas particle distribution which did not extend much beyond the radius of the OLR. The resemblance between some of the observed rings in Figs. 2–4 and those in Fig. 4 of Schwarz (1981) is very good. The time evolution of the model was such that particles near the OLR settled into periodic orbits, so that the ring preserved information on the shape and orientation of those orbits. However, Schwarz (1984a) demonstrated that a strong bar could generate an outer pseudoring aligned nearly perpendicular to the bar which lies slightly *outside* the OLR and which does not involve a settling of particles into periodic orbits. The particle distribution after six bar rotations in this model, displayed in Fig. 6 of Schwarz (1984a), includes an outer pseudoring which, like the other model, very much resembles the features seen in several of our R_1' examples. In both models the major axis radius of the outer pseudoring is still very close to the OLR, and thus in either case the ring defines the location of the resonance.

The distinguishing characteristic of the R_2' morphology is a doubling of the spiral arms in the two opposing quadrants trailing a bar or oval, owing to an $\sim 270°$ winding of the arms with respect to the ends of this feature. In this circumstance the arms clear the opposite side of the bar completely, and

therefore the morphology is easily distinguished from the R_1' type. Figures 5–7 illustrate eight examples of R_2' pseudorings, of which ESO 325 − 28, ESO 365 − 35, and ESO 577 − 3 are the most representative. One of these, ESO 365 − 35, is shown both in the middle panel of Fig. 5 and in the upper left panel of Fig. 6, the latter being based on a higher contrast setting on the television display to emphasize how the spiral arms break from near the inner lens. Since in general the arms making an R_2' can break either from the ends of a bar or from an inner ring or lens near the minor axis line of a bar, a total winding of more than 270° is possible. This type of pseudoring is probably related to the family of periodic orbits which lie just *outside* the OLR and which are aligned parallel to the bar (see Fig. 12 of Schwarz 1981). Schwarz found that a parallel-aligned pseudoring is favored in strong bar fields in general, and also in weak bar fields if there is sufficient gas beyond the OLR. This was also the most prevalent type of ring in his experiments. Several of our examples, especially ESO 325 − 28, bear a close resemblance to the model ring shown in Fig. 10 of Schwarz (1981) after five bar rotations. There are fewer examples of R_2' in the CSRG than R_1', but evaluation of the true relative frequencies is something that will require a careful statistical analysis, and will be considered in a later paper.

Figure 7 shows three somewhat unusual examples of R_2' pseudorings. The largest is that in NGC 2935, whose resemblance to the parallel-aligned family of model pseudorings was first noted by Schwarz (1984b). The galaxy has a number of nearby companions and may be slightly perturbed, since the outer pseudoring is fairly open on one side. The large, high surface brightness galaxy NGC 3358, shown in the lower panel of Fig. 7, is more symmetric but very unusual. The outer spiral pattern seems to be a promising R_2' case, but this pattern breaks far from the ends of the bar and inner lens. The galaxy NGC 4909, shown in the upper panel, displays a complex outer spiral pattern that is also a probable R_2' case.

3.2 Closed Outer Rings

From the Schwarz models, we anticipate the existence of pure (or detached) versions of the R_1' and R_2' morphologies which would be true outer rings of types R_1 and R_2. This follows from the secular evolution of the pseudoring patterns. However, it is difficult to make R_1 and R_2 assignments in practice because the more detached and uniform an outer ring is, the harder it is to fit into these categories without some independent information, such as kinematics. As a result, there are no specified cases of R_2 in the CSRG, but the situation is different for R_1 where well-defined criteria suggested by the Schwarz models can be used in some cases.

For example, we believe we can distinguish some R_1 outer rings as cases where the inner ring or oval nearly fills one axis of the outer ring, especially if the latter is slightly enhanced near the connection points. Among our sample galaxies, NGC 5728 in Fig. 4 is a good example where this criterion could be used. A very useful additional criterion for R_1 is the presence of subtle *dimples* in the zones of the ring near the axis of the bar or oval. Two cases in Fig. 4, NGC 1326 and IC 4214, show such dimples. R_1' pseudorings can also appear dimpled if the arms dip in slightly when they return to the opposing side of a bar or oval. Figure 12 of Schwarz (1981) shows that only the inner OLR orbit family is prone to such dimpling for the conditions in his models, the dimples representing regions where the tangential velocity comes close to zero in the rotating frame. The time sequence in Schwarz's Fig. 4 shows that the outer gas ring which forms after ten bar rotations retains this dimpling.

It is noteworthy that in some galaxies where we recognize a clear R_1 ring, this ring is imbedded within an obvious extended disk whose isophotal shape differs from the shape of the ring. Such an outer disk is very conspicuous in IC 4214 and in ESO 437 − 33 (Fig. 9). There is material beyond the outer ring of NGC 1326 in the form of weak spiral arms, but little is evident in the case of NGC 5728 (as seen on the SRC sky survey, since our image of this galaxy covers a limited field). These outer disks serve to highlight the fact that, in general, R_1 rings are probably not intrinsically circular.

3.3 The $R_1 R_2'$ Morphology

It was pointed out by Buta (1986) that some galaxies show a complex outer spiral pattern which contains aspects of both an R_1 and an R_2' morphology. The CSRG galaxies ESO 509 − 98 and ESO 507 − 16 provide two of the best displays of this combined pattern, which we call R_1R_2'. Figures 8 and 9 display them and several others. In ESO 509 − 98, there is a very good R_2' pseudoring pattern, but this pattern does not break from the bar or an inner ring or a lens. Instead, the R_2' pattern could be interpreted as breaking from a second outer ring which is mostly detached, thin, and slightly dimpled (see Fig. 1 schematic, and also the upper right panel of Fig. 6 which displays a higher contrast image than that in Fig. 8). We interpret this inner feature as an R_1 component. A noteworthy characteristic is that the R_2' part appears to break from the R_1 part near a line perpendicular to the bar axis. The two ring features of ESO 509 − 98 are so conspicuous on the SRC sky survey plate of the field that the galaxy was catalogued by Arp and Madore (1987) with the following comment: "Spiral with double ring arms."

In ESO 507 − 16, the inner R_1 component is more conspicuous than in ESO 509 − 98, but the R_2' component does not close well. A notable feature is the dimpling of the R_1 component, especially on one side (see the higher contrast image in the upper right panel of Fig.9). In the CSRG, any galaxy showing spiral structure breaking from a clear outer ring in the manner displayed by ESO 507 − 16 is assigned to the R_1R_2' category. In most cases, one or the other of the two components is dominant rather than both being equally conspicuous. For example, in NGC 3482 (Fig. 8) and ESO 426 − 2 (Fig. 9), the R_1 component is dominant, while in ESO 365 − 35, we suspect only a trace of R_1 within a dominant R_2'.

As in Buta (1986, 1989), we interpret the R_1R_2' morphology as the unexpected manifestation of both Schwarz (1981) OLR ring patterns. If, for example, the inner OLR ring which developed after ten bar rotations in Schwarz's Fig. 4 is superposed within the outer OLR pseudoring which developed after seven bar rotations in Schwarz's Fig. 10, then a combined pattern emerges which resembles the R_1R_2' morphology. However, our interpretation is controversial because as shown in Schwarz's Fig. 12, the two OLR orbit families intersect. This intersection precluded the coexistence of the two rings in Schwarz's dissipational models. On the other hand, there is no better interpretation of the R_1R_2' morphology than in terms of the OLR, and future improved

simulations may be able to clarify under what circumstances the coexistence might be possible.

4. DISCUSSION

The galaxies in the present sample were mostly chosen on the basis of outer ring or pseudoring morphology and not on the stage (S0, Sa, Sb, etc). or family (barred versus nonbarred) classification. The images have revealed a wealth of interesting details on bar morphologies, dust lane patterns, and nuclear structures whose relationship to the outer patterns have rarely had the benefit of a systematic study. In this section we discuss correlations between the structures seen in the inner regions of our sample galaxies and outer ring/pseudoring morphologies, realizing that our sample is too small for definitive conclusions. More specific details concerning inner features, especially nuclear and inner rings, will be analyzed in a separate paper.

4.1 Hubble Types

It is clear from Table 1 that our sample emphasizes early type spirals: the average stage is Sa with only a small range (S0/a to Sb). This implies, in general, that the galaxies are not gas rich and that they are likely to be massive. In the CSRG as a whole, there are actually very few late-type (Sc-Sm) examples, which again may reflect the influence of both total mass and gas fraction on the development of these features.

It is also clear from Table 1 that our sample emphasizes barred galaxies: only 2 of the 22 objects displaying one of the OLR ring morphologies in Fig. 1 can be classified as SA, and both of these (IC 4214 and NGC 4909) have an obvious oval. An important finding made by Schwarz was that the parallel-aligned OLR morphology was more likely to develop than the perpendicular OLR morphology if the bar field at the OLR is strong or if the bar is weak and there is gas beyond the OLR. Thus, we might expect that galaxies where the R_1' morphology is prominent might be classified more often as SAB types or have more centrally concentrated bars compared to those showing the R_2' morphology. If we examine family classifications in Table 1 within the R_1' and R_2' subclasses, only a small difference emerges: the average bar classification is SAB for the R_1 and R_1' types, and SAB for the R_2' types. Though we certainly cannot assess true bar strength reliably from family classifications, it could be an important contradiction to the theory if apparently strong bars are more frequent in the R_1 or R_1' cases. The referee has correctly pointed out that comparisons of apparent bar strength between the two OLR subclasses could be influenced by projection effects, especially if one attempts to deproject the galaxies assuming circular symmetry of the pseudorings. Only a much larger sample could clarify the issue.

Another aspect of the types is that nearly 80% of the sample galaxies are double ringed, showing both inner and outer ring or pseudoring features. At least five of the objects (NGC 1326, ESO 565 – 11, ESO 437 – 67, IC 4214, and NGC 5728) are triple-ringed, showing inner, outer, and nuclear rings or pseudorings. In general, these galaxies present some of the most complex morphologies among the normal galaxy population. In only four cases would the outer rings qualify for classification in the Hubble–Sandage system (column 6 in Table 1).

4.2 Bar Morphologies

We can ask next whether bar morphologies show any correlation with the appearance of the outer ring or pseudoring. In Table 1, we refer to standard SB-type bars as "regular" bars. These appear in a wide range of contrasts so that some are classified as SB and others SAB, but near stage Sb they often have prominent linear dust lanes (Sandage 1961) that are revealed clearly on the color index maps (see next section). In contrast, many bars in early-type galaxies have bright enhancements ("ansae") near the ends that give them the appearance of a dumbbell. In Sandage (1961) and the RSA, an SB0 with an ansae-type bar is classified as $SB0_2$, while in Buta (1986) such bars were referred to as "three-blob" types (with the nucleus counting as one blob). Ansae bars are also found among early type spirals, and in the present sample there are two clear examples: ESO 509 – 98 and NGC 3358. In both cases the blobs are short arcs. In ESO 507 – 16, the inner ring has bright enhancements near its major axis that seem obviously related to an ansae-type bar. In all three of these objects, an R_2' pseudoring is prominent. Other objects in the sample where the bar shows some ansae character are NGC 1326, ESO 360 – 15, NGC 2983, ESO 566 – 24, and NGC 3482, implying that this character is detectable from stages S0 to Sb. In some of these an R_1 or R_1' feature is prominent, so there tentatively does not appear to be a clear correlation between bar type and the appearance of the outer ring or pseudoring.

4.3 Dust Lane Morphologies

The color index maps reveal some very interesting dust lane patterns in the bar regions of 11 of the sample galaxies. The morphology of bar dust lanes has been considered recently by Athanassoula (1984, 1988), who demonstrated how bar strength and the existence of an inner Lindblad resonance help to shape these features. She identified three major dust lane types among the regular bars: type *a* lanes are the most linear while type *c* lanes are the most curved. Type *b* lanes are straight along the bar but curve in the vicinity of the core, hence are intermediate between types *a* and *c*. Column 8 of Table 1 assigns these types, where relevant, on the basis of the color maps. The weaker bars appear to have the most curved or complex dust lanes. This is especially true in NGC 1326, where the dust lane pattern is regular but extremely unusual. Near the ends of the weak bar, the dust lanes curve sharply, and in the intermediate regions of the bar there are two extra, highly curved lanes. No model of a barred galaxy has predicted anything like this pattern.

Of the 11 galaxies in our sample where a dust lane pattern is clearly distinguishable within the region covered by a bar or inner oval, nine have outer rings or pseudorings which we have placed into the R_1 or R_1' categories (including ESO 566 – 24; see Fig. 10). The remaining two are ESO 565 – 11 (Fig. 11), where the possible lanes are only weakly evident in the *B*-band image, and NGC 2935, the only R_2' case. Fifteen of the sample objects within the OLR subset show only weak or no clear dust lane pattern at all. Of these, four are R_1', three are R_1R_2', and eight are R_2' cases. A dependence on Hubble type could possibly explain these findings, since it is well known (Sandage 1961) that bar dust lanes are prominent near stage Sb.

4.4 Nuclear Structures

The color maps in Figs. 2–13 show the interesting character of the distribution of star formation in ringed galaxies. Whenever a ring is conspicuous in blue light, it also appears as a blue enhancement in these maps. The relationship with spiral structure, which usually outlines star-forming regions, is obvious, but most interesting are the nuclear structures. Fourteen of the sample galaxies show evidence for nuclear star formation, nine in the form of small rings and five in the form of blue nuclei or partial rings. In Table 1, a nuclear ring is part of the classification in column 5 *only* if it is clearly distinguishable in the blue light image (to preserve the basis of the classification). This was true in the six cases (NGC 1326, NGC 2935, ESO 565 – 11, ESO 437 – 67, IC 4214, and NGC 5728) where the symbol nr is used in the type, while in the remaining three cases (ESO 437 – 33, ESO 566 – 24, and ESO 507 – 16) a nuclear ring is only distinguishable in the color index map.

It is interesting to note that of the six R_1' galaxies in Figs. 2 and 3, five contain nuclear star formation: NGC 2665, ESO 508 – 78, ESO 437 – 67, NGC 3504, and ESO 360 – 15. The same is true for the R_1 cases: all three of the objects in Fig. 4 show clear nuclear rings, the one in NGC 1326 being especially intense. To these we must add ESO 437 – 33, where the main outer ring feature is a virtually closed R_1. The galaxies having the R_1 outer ring/ pseudoring types but which do not show any nuclear star formation are ESO 575 – 47 and ESO 426 – 2; both also show no evidence for dust within an inner ring. Thus, *9 out of 11 examples chosen on the basis of the* R_1 *or* R_1' *outer ring or pseudoring morphology display clear evidence for nuclear star formation.* Three additional cases in Table 1, ESO 566 – 24 (Fig. 10), NGC 5134 (Fig. 12), and IC 4290 (also Fig. 12) may belong to this subset but are less clearcut examples; they are described in the appendix. With them the proportion would be 10 out of 14.

In contrast, the color distributions in the eight R_2' cases in Figs. 5–7 demonstrate that nuclear star formation is less frequent. Only two of these eight objects show evidence for such star formation: ESO 325 – 28 and NGC 2935. If we consider the three R_1R_2' cases in Fig. 8 where the R_2' morphology is prominent, only one, ESO 507 – 16, shows weak evidence for circumnuclear star formation. Thus, *8 of 11 galaxies displaying the* R_2' *morphology show no evidence for nuclear star formation.*

4.5 Local Environments

The local environments of the galaxies in Table 1 are of interest because no systematic study has yet been made of the frequency of companions to such galaxies. This is a subject which will be addressed with the full CSRG later, but as an indication of what to expect we have examined the fields of all of the galaxies in Table 1 on the charts of the SRC-J or the ESO-R southern sky surveys. No galaxy in our sample lies in a rich cluster environment, though several are in the outskirts of clusters: NGC 1326 and IC 1993 (Fornax); ESO 501 – 51 (Hydra I); and NGC 4553 (Centaurus). The latter three objects are described in the Appendix. Two of our R_2' galaxies are in compact groups: NGC 3269 and NGC 3358. Both are peculiar to some extent, and NGC 3269 shows a faint feature at very low surface brightness (not evident in Fig. 6) suggestive of interaction. The remaining galaxies have one or several comparable companions nearby in sparse groupings or are on charts with many galaxies. In the cases of NGC 2665, ESO 565 – 11, NGC 2983, IC 4290, and NGC 4909, comparable companions are more than 15 outer ring diameters away. The tentative indication is that our galaxies lie in relatively average environments, neither unusually high nor unusually low in galaxy density.

5. CONCLUSIONS AND FUTURE WORK

We have presented a detailed atlas of images and color distributions in 30 galaxies from the Catalogue of Southern Ringed Galaxies classified as having outer rings and pseudorings. Of these, 22 were chosen because the morphology resembles that of *n*-body model rings which develop near the outer Lindblad resonance. We have attempted to demonstrate that some of the morphological details discovered in the *n*-body models of Schwarz (1981) can be identified in real galaxies and moreover in a substantial number of galaxies. The observed characteristics of our sample rings support Schwarz's suggestion that the OLR is a dominant factor in the morphology of barred galaxies and that the outer rings and pseudorings of such galaxies may be identified with this resonance. Regardless of this interpretation, we have also demonstrated that distinct morphological subclasses do exist among the outer rings and pseudorings of normal galaxies, and that there are other structural correlations that may accompany these subclasses with regard to apparent bar strength, presence of global dust lanes in the bar region, and nuclear star formation.

The next steps in this study are (1) to increase the sample of observed objects considerably to strengthen its statistical significance, and (2) to process the CCD images to derive more objective morphological and photometric data. These data will be used to guide new numerical simulations and evolutionary synthesis of colors in order to extend Schwarz's work and to establish more clearly the role of secular evolution and bars in the creation of these exotic and interesting ring morphologies. Using outer rings and pseudorings to indirectly estimate pattern speeds will require further work as well, since these features are so faint that kinematic information will not necessarily be easy to obtain. An additional important problem is the undoubtedly noncircular intrinsic shapes of these features. A morphological survey is planned of all galaxies with published HI or optical rotation curves to see how many show the R_1' and R_2' morphologies. New kinematic observations of some of the galaxies in Table 1 are also planned. A detailed discussion of problems associated with pattern speeds is given by Sellwood and Sparke (1988).

R.B. would like to thank M. P. Schwarz and A. J. Kalnajs for useful discussions and for stimulating and encouraging the production of the CSRG. He would also like to thank G. de Vaucouleurs and H. Corwin, Jr. for further encouragement and support over the seven years the CSRG has been in progress, and an anonymous referee for some helpful comments. This research was supported in part by NSF/ EPSCoR Grant No. RII 8996152 and by NSF Grant No. AST 9014137 to the University of Alabama.

APPENDIX: SPECIAL CSRG CASES

A survey like the CSRG has great value not only for statistics and follow-up studies of a phenomenon like rings, but

also for the identification of cases of special interest. Figures 10–13 display eight such cases, the most interesting of which is ESO 566 – 24 (Fig. 10). This remarkable object, which may look rather plain at first, is one of the most regular examples of a four-armed ringed barred spiral in the sky. None of the major catalogs covering the CSRG zone makes any note of this characteristic. Three images: *B*, *I*, and *U*, and a $B - I$ color index map, are displayed. The inner ring is nearly circular and evidently very blue, and the images show that the four arms break from the ring in a symmetric pinwheel pattern that is especially regular in the *I* band. The arms form a four-leaf clover style outer pseudoring that is rare in the CSRG, and the pair of arms breaking from near the ends of the bar would probably be classified as an R_1' if they existed alone. The pattern is reminiscent of NGC 1433, a bright SB(r)-type spiral showing two outer arms and two isolated arcs off the leading sides of the bar which Buta (1984) called "plumes." We have attempted to deproject ESO 566 – 24 assuming the outer disk is circular, and find a resulting pattern very similar to NGC 1433 with the two side arms representing the "plumes." This suggests that the "plumes" in NGC 1433 are related to this four-arm morphology. The arcs in that case may appear isolated owing to the rather stronger than average bar. The $B - I$ color index map reveals a small, partial nuclear ring in ESO 566 – 24, as well as straight bar dust lanes.

A fascinating CSRG galaxy that cannot be fit easily into any of the OLR categories is ESO 565 – 11 (Fig. 11). This galaxy shows an unusual bar resembling a candle-pin (from bowling terminology: fat in the middle, narrower near the ends, and flat at both ends). A faint, slightly asymmetric pseudoring breaks perpendicularly from the sharp and straight ends of this bar. The upper right panel in Fig. 11 shows a deeper image and reveals two faint spiral arms beyond the pseudoring. We therefore interpret the unusual pseudoring wrapping the bar as of the inner (rs) type. Unfortunately, a bright star scattered light into the frame and affects half the galaxy, making it difficult to evaluate the full nature of the outer structure. The two outer arms may in fact form an outer pseudoring. The most interesting aspect of this galaxy is the very bright circumnuclear ring of blue knots. The ring is overexposed on both the SRC-J and ESO-R survey charts of the field, and is unusually large compared to the size of the galaxy. The ring is also significantly elongated and displays a slightly oblique angle with respect to the leading edges of the bar. This galaxy stands apart from the others in the sample.

The three galaxies displayed in Fig. 12 are barred with distinctive characteristics. The top panel shows IC 4290, which has a high contrast inner ring enveloping an exceptional bar. We see evidence for boxiness in the inner part of the bar, but it is interesting that there is no trace of nuclear or circumnuclear star formation. Virtually all of the recent star formation in IC 4290 is taking place in the inner ring. The structure outside the inner ring is very faint, and appears to be a two-armed low contrast spiral pattern which breaks from the ring near the minor axis line of the bar. The pattern appears to wind only about 180° with respect to the ends of the bar, and thus favors an R_1' interpretation.

The middle panel of Fig. 12 shows NGC 2983, a well-known SB0 galaxy with a clean bar and a bright outer, mostly uniform disk. We display this object because it has an excellent example of an "outer lens", a type of feature discussed by Kormendy (1979). The revised classification is $(L)SB(s)0^+$, where the (L) notation was suggested by Kormendy. It is very likely that the (L) in NGC 2983 is related to an outer ring, or perhaps once was an outer ring.

The bottom panel of Fig. 12 shows the inner regions of the large outer-ringed galaxy NGC 5134. The ring is very faint and was too large for the field of the CCD; it will be imaged later with a large format CCD. On the SRC-J copy film of the field, the outer ring is smooth and nearly circular, but is filled along one dimension by the inner zone. Thus, the ring could be an R_1 type. What makes the galaxy interesting is that the inner zone includes a highly elongated patchy oval which could be interpreted as an SAB-type bar. However, within the oval we see a clear bar much like that in NGC 3504, especially in the *I* band, which suggests that the patchy oval is an unusually intrinsically elongated inner ring. The color index map shows that the patchy oval is blue near the rim, much like typical inner rings. We classify NGC 5134 as $(R_1)SAB(rl)ab$, but it is an example of this type with little or no clear spiral structure.

In Table 1, our assignment of the de Vaucouleurs family classification (i.e., SA, SAB, SB) refers mainly to bars and not ovals. For example, the galaxies IC 4214 and NGC 4909 have clear ovals but no trace of a conventional bar, therefore we classify them as SA. Figure 13 displays three typical SA ringed galaxies (NGC 4553, IC 1993, and ESO 501 – 51) from the CSRG which do not contain obvious ovals, to show how the ring features compare in morphology to the more typical examples in the other figures. The morphological details discussed in the previous sections cannot be applied effectively in these SA cases, and we cannot make unambiguous resonance identifications on the basis of morphology alone. Judgments can, however, be made on the basis of the size ratio of an inner and outer ring if both are present (Athanassoula *et al.* 1982).

The most interesting case in Fig. 13 is NGC 4553, an example with a conspicuous inner ring and a faint outer disk classified as an outer ring in Corwin *et al.* (1985). The contrast of the outer ring is low, however, and no ring character is evident on our CCD images. The color index map shows a weak color enhancement in the inner ring and little dust. An important feature revealed by our new images is a tiny bar in the bulge, less than one-sixth the size of the inner ring. This should be compared with an interesting counterpart, NGC 7702, which is of the same type as NGC 4553 and which also contains a small nuclear bar (Buta 1991b).

IC 1993 is interesting because on the SRC chart of the field, this galaxy resembles a planetary nebula with a nearly circular ring. Our images show that the apparent ring is a pseudoring made of three or four arms. The galaxy is almost a pure spiral of late type, but the color index map shows that star formation is definitely concentrated in a ring near the edge of the bright inner disk. Finally, ESO 501 – 51 is a bright SA galaxy with double (inner and outer) pseudoring structure near the well-known Hydra I galaxy cluster.

REFERENCES

Arp, H. C., and Madore, B. F. 1987, A Catalogue of Southern Peculiar Galaxies and Associations (Cambridge University Press, Cambridge), Vol. I

Athanassoula, E. 1984, Phys. Rep., 114, 319

Athanassoula, E. 1988, in Proceedings of the Joint Varenna-Abastumani International School on Plasma Astrophysics (ESA-SP285), Vol. 1, p. 341

Athanassoula, E., Bosma, A., Creze, M., and Schwarz, M. P. 1982, A&A, 107, 101

Buta, R. 1984, PASAU, 5, 472

Buta, R. 1986, ApJS, 61, 609

Buta, R. 1989, in The World of Galaxies, edited by H. G. Corwin and L. Bottinelli (Springer, New York), p. 29

Buta, R. 1990, ApJ, 356, 87

Buta, R. 1991a, in Dynamics of Galaxies and Their Molecular Cloud Distributions, IAU Symposium No. 146, edited by F. Combes and F. Casoli (Kluwer, Dordrecht), p. 251

Buta, R. 1991b, ApJ, 370, 130

Buta, R., and Crocker, D. A. 1991, in preparation

Corwin, H., de Vaucouleurs, A., and de Vaucouleurs, G. 1985, Southern Galaxy Catalogue (University of Texas Monographs in Astronomy No. 4, Austin)

de Vaucouleurs, G. 1959, Handbuch der Physik, 53, 275

de Vaucouleurs, G., de Vaucouleurs, A., and Corwin, H. 1976, Second Reference Catalogue of Bright Galaxies (University of Texas Press, Austin)

de Vaucouleurs, G., de Vaucouleurs, A., Corwin, H., Buta, R., Paturel, G., and Fouque, P. 1991, Third Reference Catalogue of Bright Galaxies (Springer, New York)

Kormendy, J. 1979, ApJ, 227, 714

Lauberts, A. 1982, The ESO-Uppsala Survey of the ESO (B) Atlas (European Southern Observatory, Munich)

Sandage, A. 1961, The Hubble Atlas of Galaxies (Carnegie Institution of Washington Publication No. 618, Washington)

Sandage, A., and Bedke, J. 1988, Atlas of Galaxies Useful for the Cosmological Distance Scale (NASA, Washington)

Sandage, A., and Tammann, G. A. 1987, A Revised Shapley–Ames Catalog of Bright Galaxies (Carnegie Institution of Washington Publ. No. 635, Washington)

Schwarz, M. P. 1981, ApJ, 247, 77

Schwarz, M. P. 1984a, MNRAS, 209, 93

Schwarz, M. P. 1984b, private communication

Sellwood, J. A., and Sparke, L. S. 1988, MNRAS 231, 25P

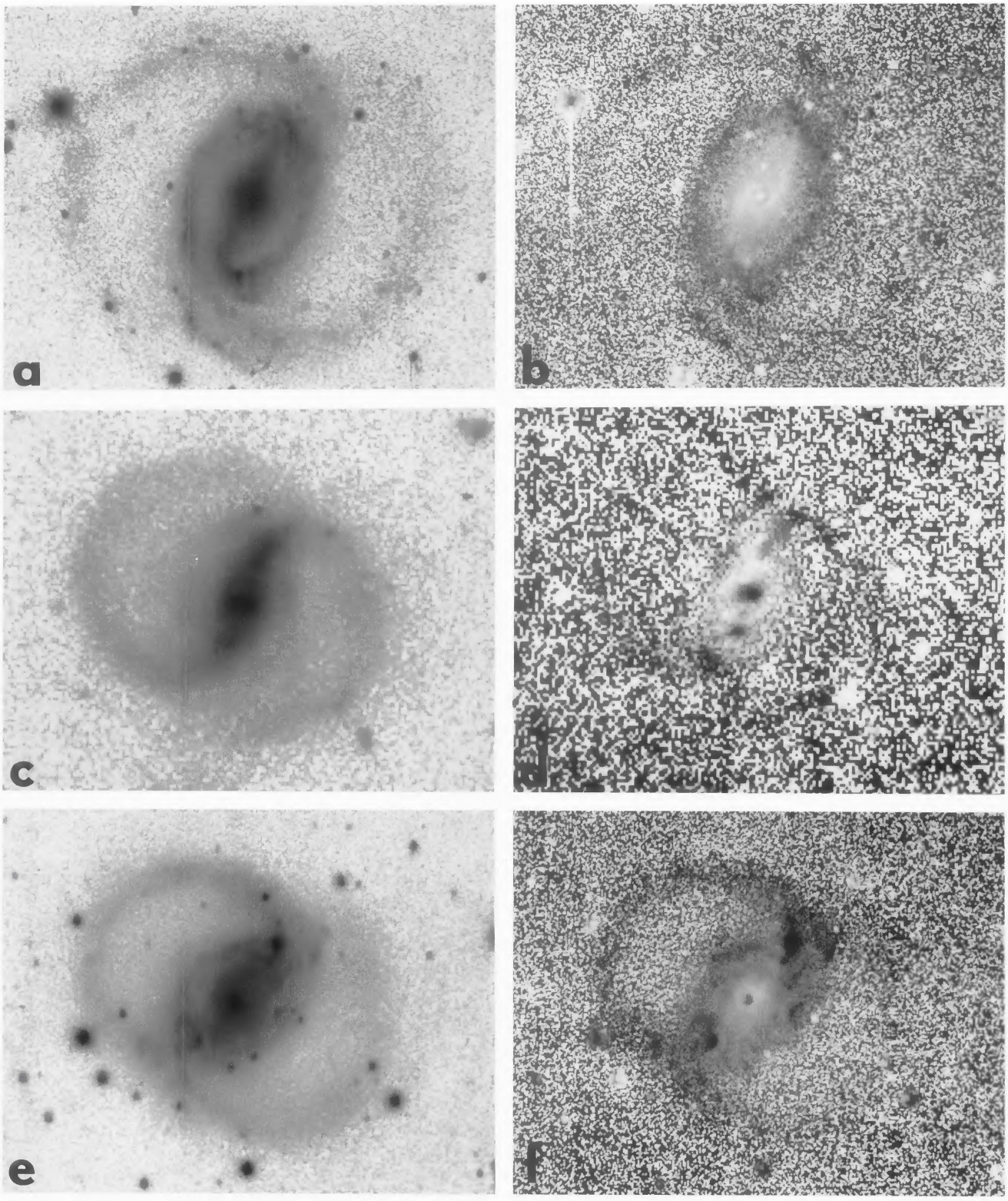

FIG. 2. Examples of R_1' pseudorings: (a) ESO 437 − 67 (B); (b) ESO 437 − 67 ($B - I$); (c) ESO 508 − 78 (V); (d) ESO 508 − 78 ($B - I$); (e) NGC 2665 (B); (f) NGC 2665 ($B - I$).

R. Buta and D. A. Crocker (see page 1718)

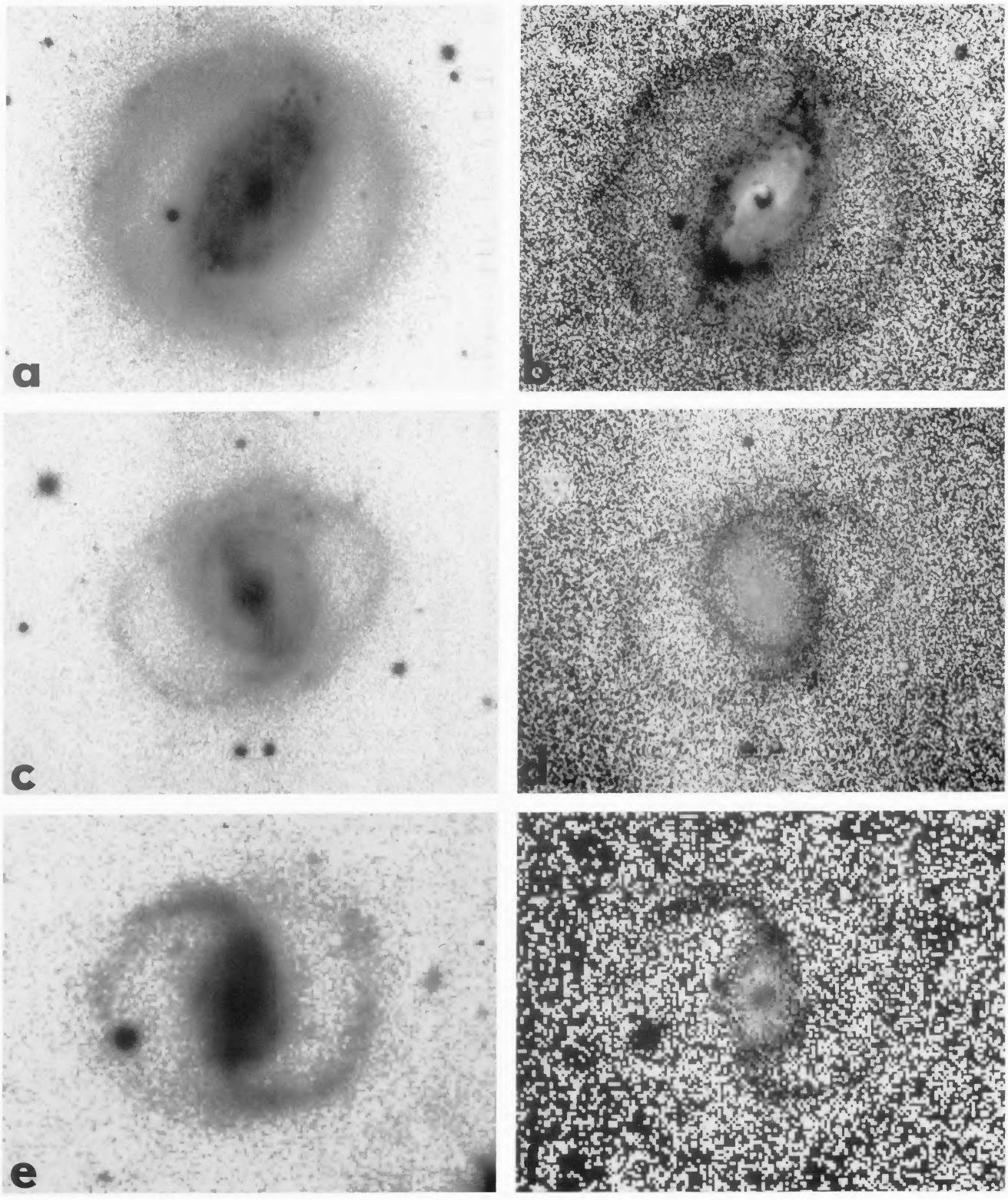

FIG. 3. Examples of R_1' outer pseudorings: (a) NGC 3504 (B); (b) NGC 3504 ($B-I$); (c) ESO 575 − 47 (B); (d) ESO 575 − 47 ($B-V$); (e) ESO 360 − 15 ($B+V$); (f) ESO 360 − 15 ($B-I$)

R. Buta and D. A. Crocker (see page 1718)

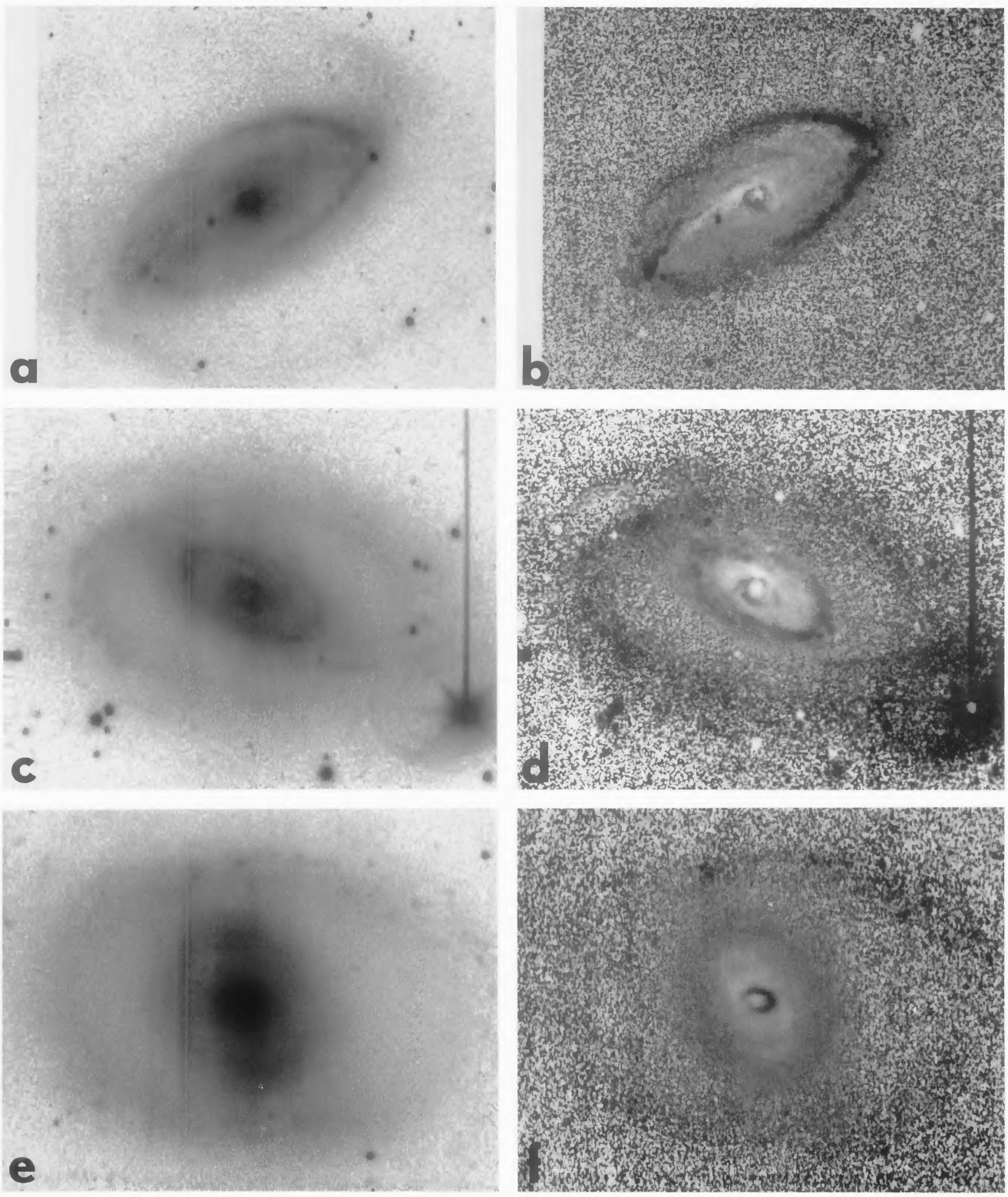

FIG. 4. Examples of R_1 outer rings: (a) NGC 5728 (B); (b) NGC 5728 ($B-I$); (c) IC 4214 (B); (d) IC 4214 ($B-I$); (e) NGC 1326 (B); (f) NGC 1326 ($B-I$).

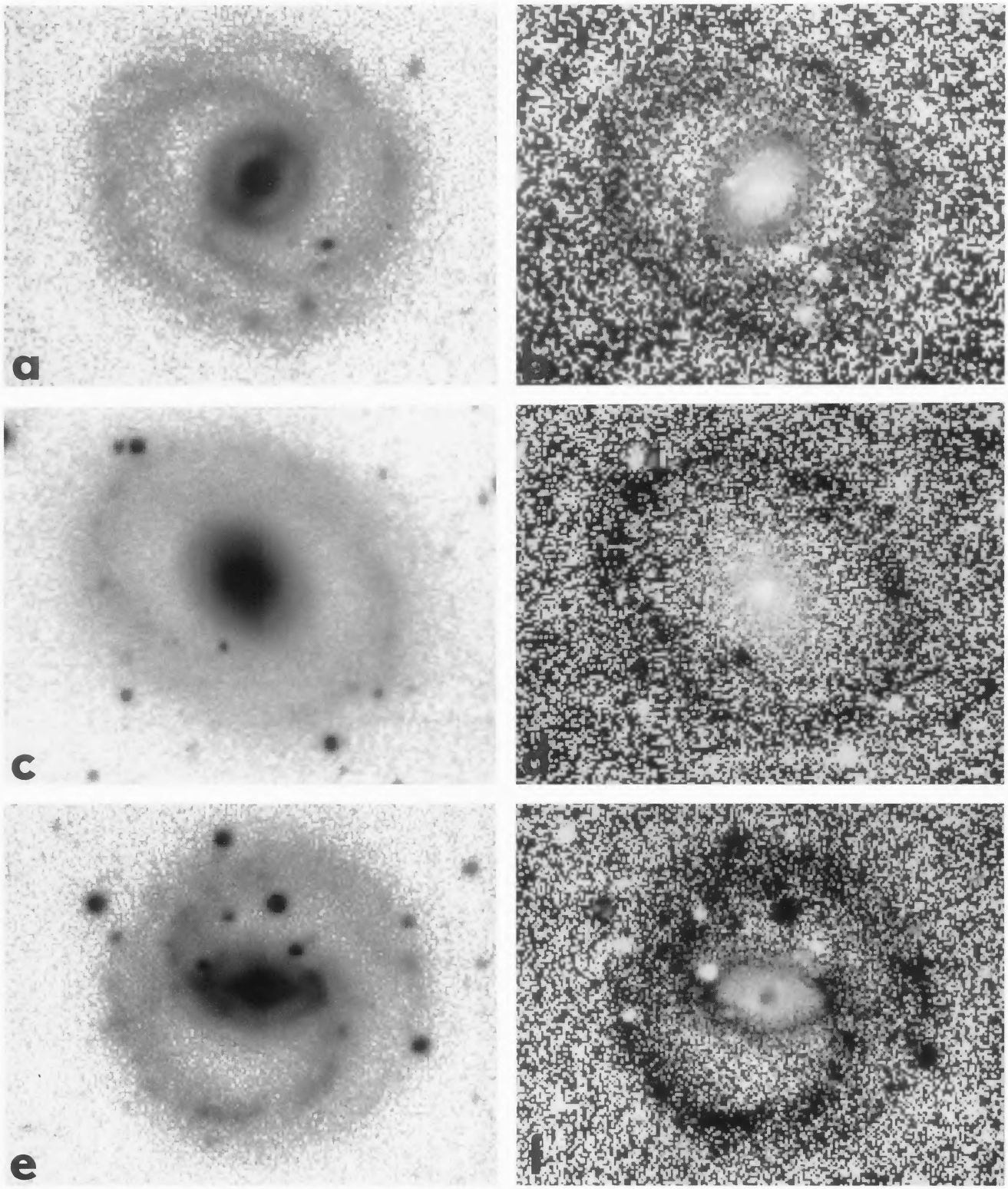

FIG. 5. Examples of R_2' outer pseudorings: (a) ESO 577 − 3 (B); (b) ESO 577 − 3 ($B - I$); (c) ESO 365 − 35 [B; see also Fig. 6(a)]; (d) ESO 365 − 35 ($B - I$); (e) ESO 325 − 28 (B); (f) ESO 325 − 28 ($B - I$).

R. Buta and D. A. Crocker (see page 1718)

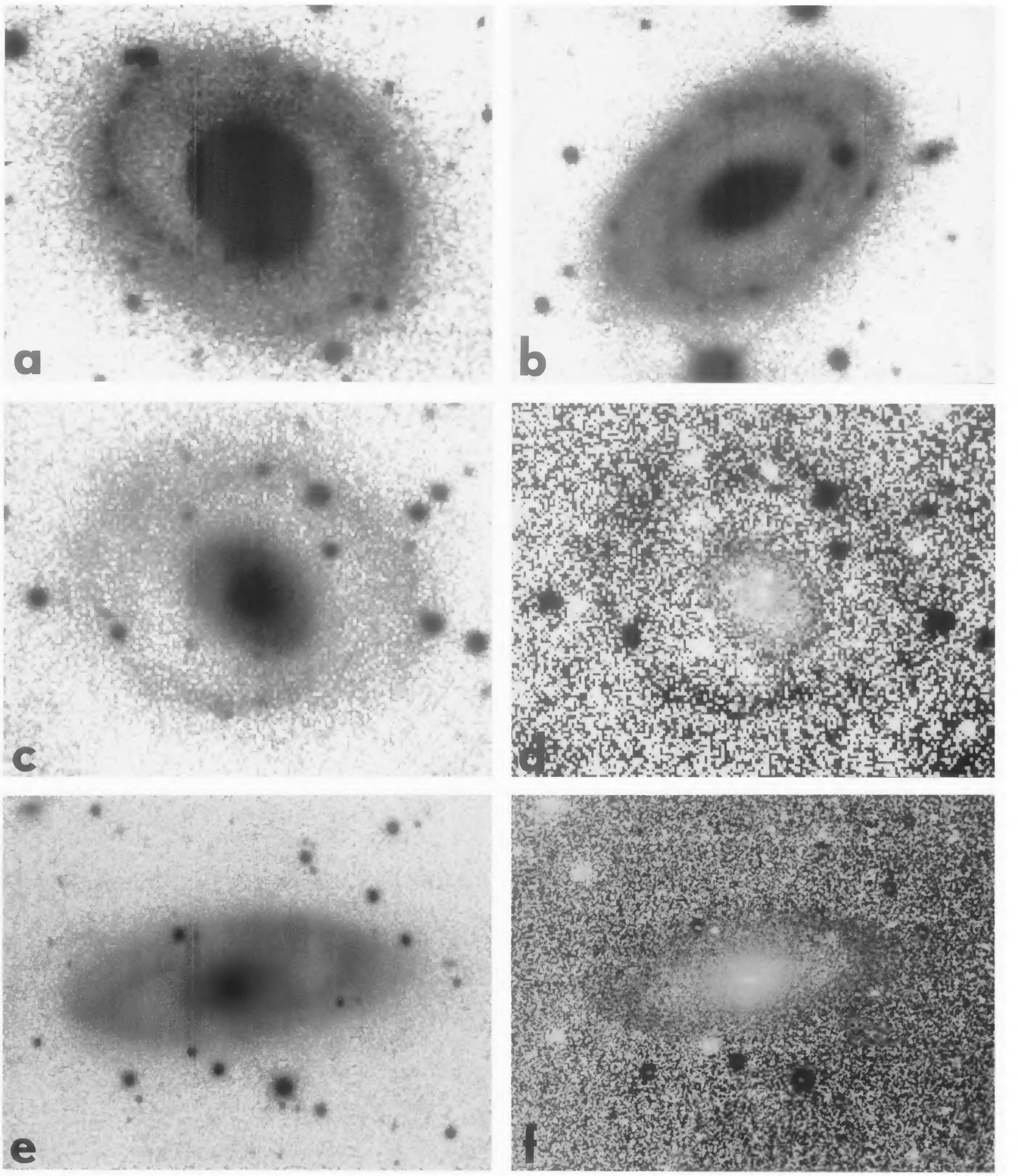

FIG. 6. Examples of R_2' outer pseudorings: (a) ESO 365 − 35 [*B*; see also Fig. 5(c)]; (b) ESO 509 − 98 [*B*; see also Fig. 8(e)]; (c) ESO 264 − 47 (*B*); (d) ESO 264 − 47 (*B* − *I*); (e) NGC 3269 (*B*); (f) NGC 3269 (*B* − *I*).

R. Buta and D. A. Crocker (see page 1718)

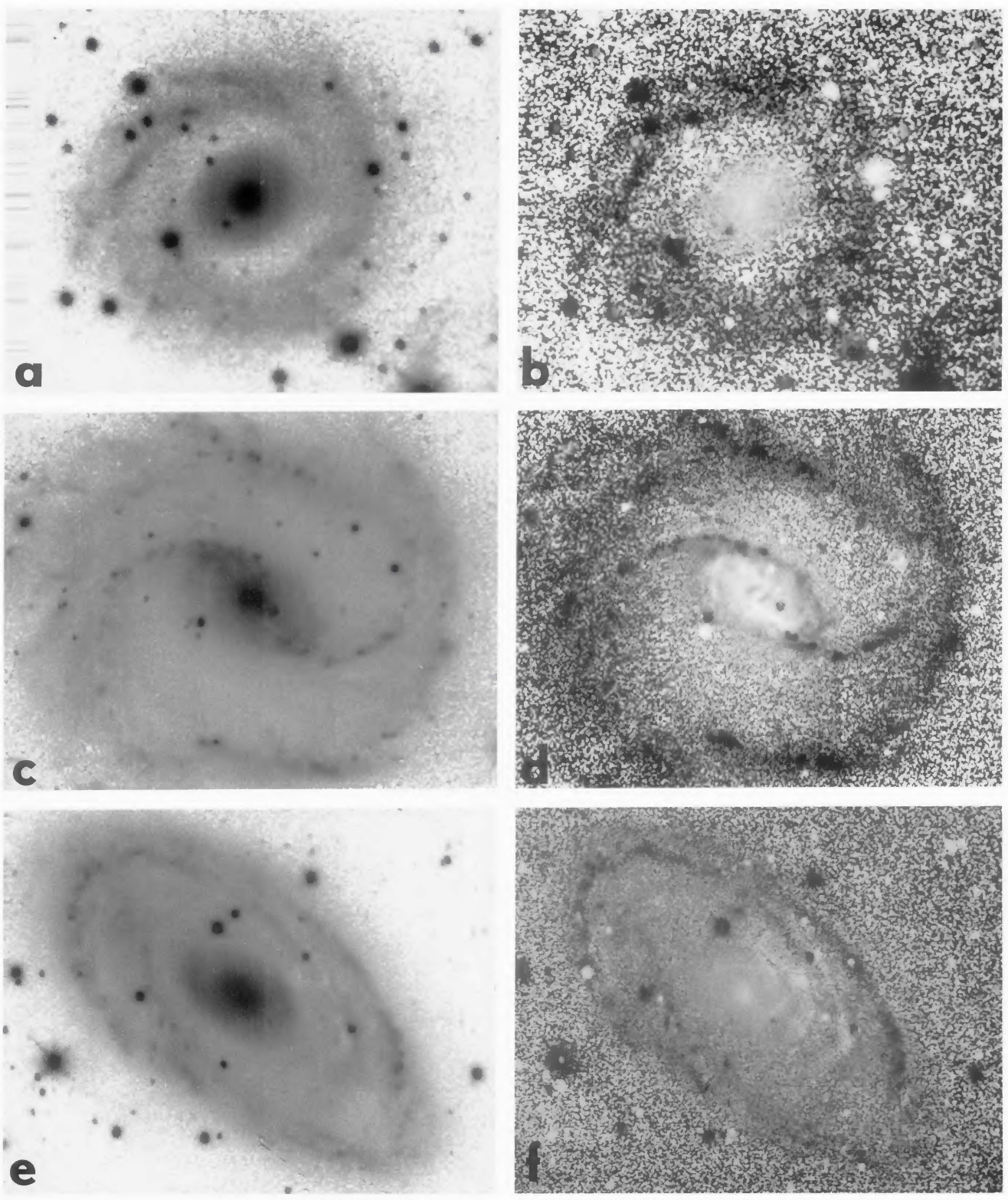

FIG. 7. Examples of R_2' outer pseudorings: (a) NGC 4909 (B); (b) NGC 4909 ($B-I$); (c) NGC 2935 (B); (d) NGC 2935 ($B-I$); (e) NGC 3358 (B); (f) NGC 3358 ($B-I$).

R. Buta and D. A. Crocker (see page 1718)

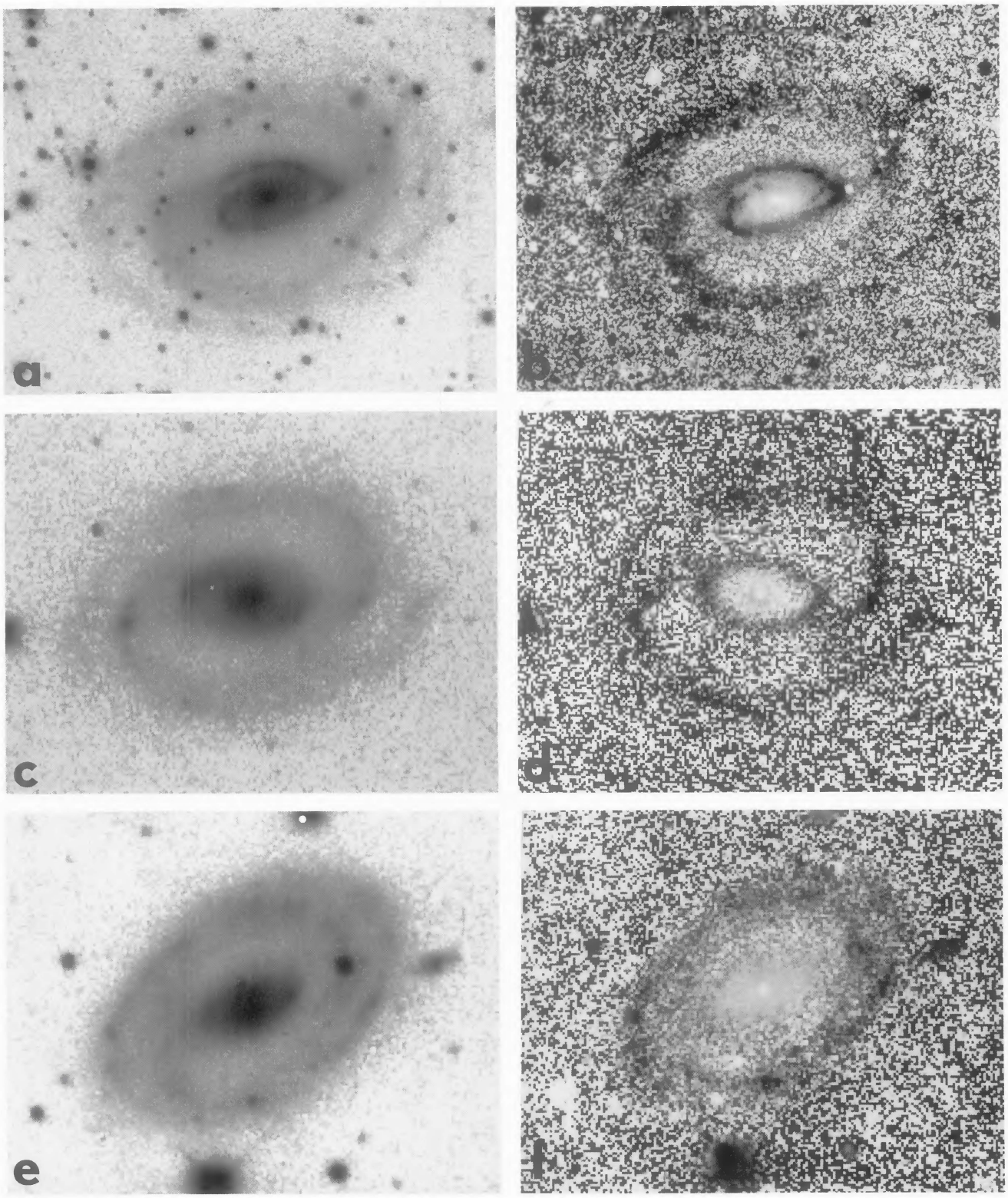

FIG. 8. Examples of R_1R_2' outer pseudorings: (a) NGC 3482 (B); (b) NGC 3482 ($B-I$); (c) ESO 507 − 16 (V); (d) ESO 507 − 16 ($B-I$); (e) ESO 509 − 98 [B; see also Fig. 6(b)]; (f) ESO 509 − 98 ($B-I$).

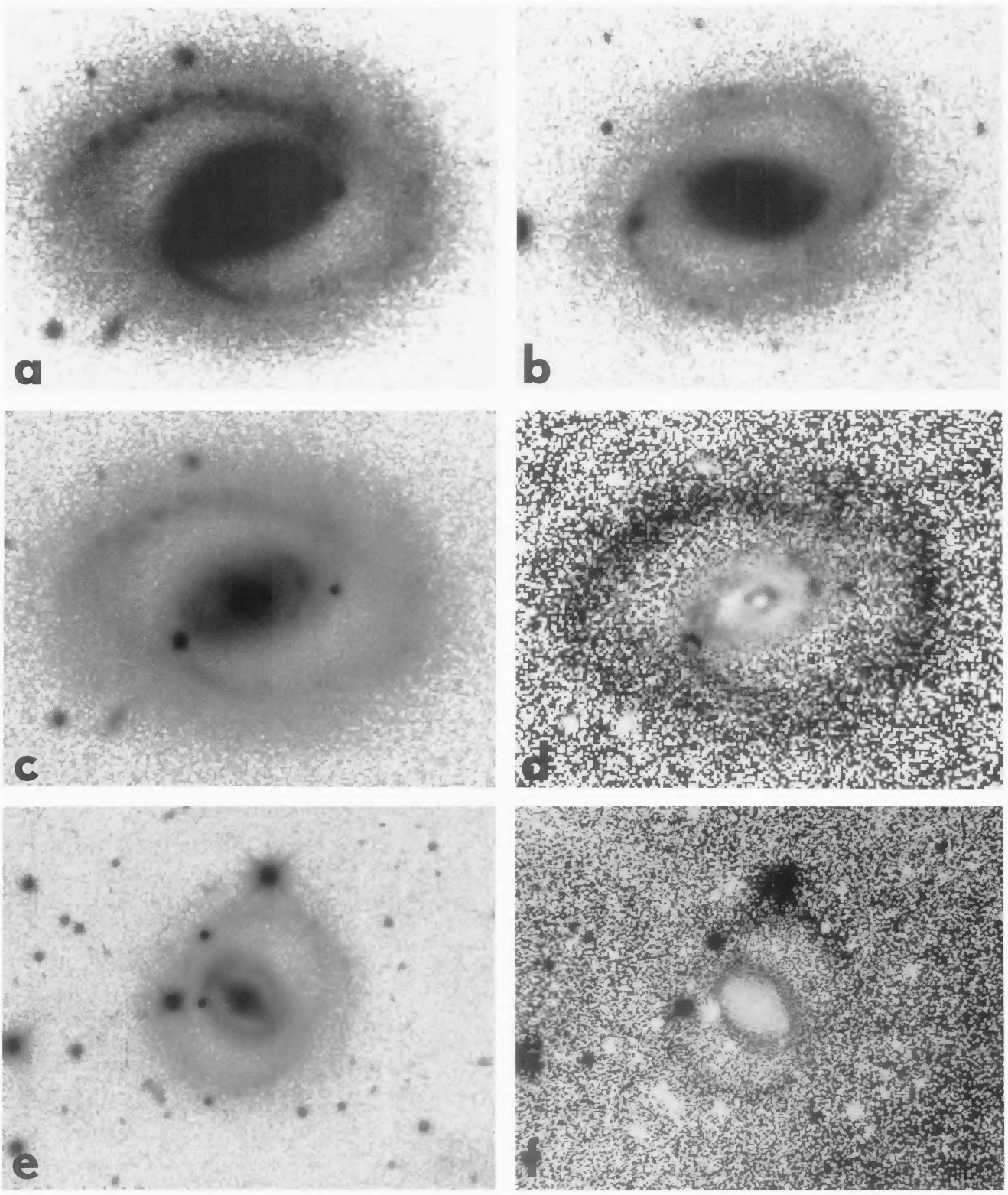

FIG. 9. Examples of R_1R_2' outer pseudorings and a related case: (a) ESO 437 − 33 (*B*); (b) ESO 507 − 16 [*V*; see also Fig. 8(c)]; (c) ESO 437 − 33 (*B*); (d) ESO 437 − 33 (*B* − *I*); (e) ESO 426 − 2 (*B*); (f) ESO 426 − 2 (*B* − *I*).

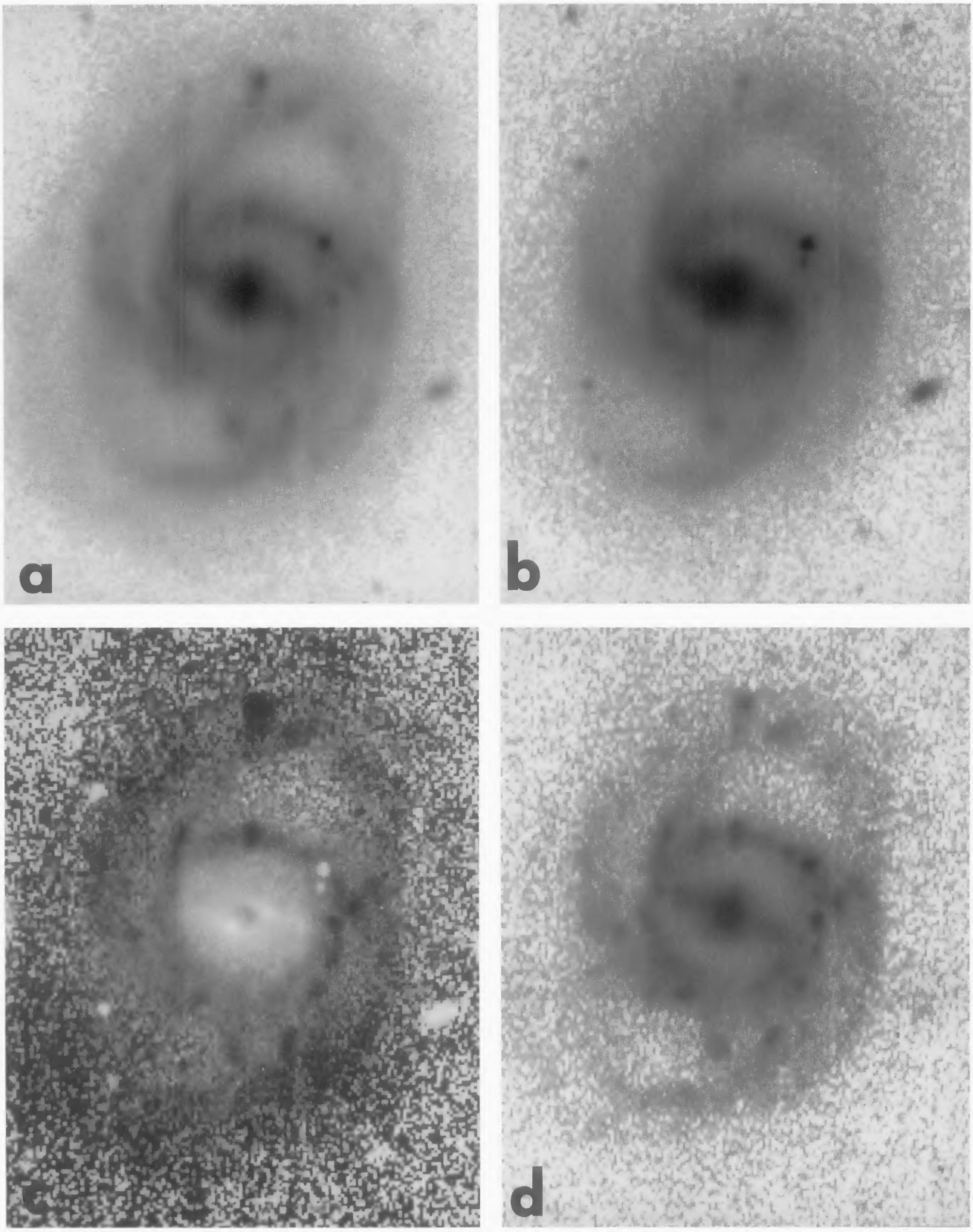

FIG. 10. ESO 566 — 24, the most prominent four-armed ringed barred spiral in the CSRG. Images: (a) B; (b) I; (c) $B - I$; (d) U.

R. Buta and D. A. Crocker (see page 1718)

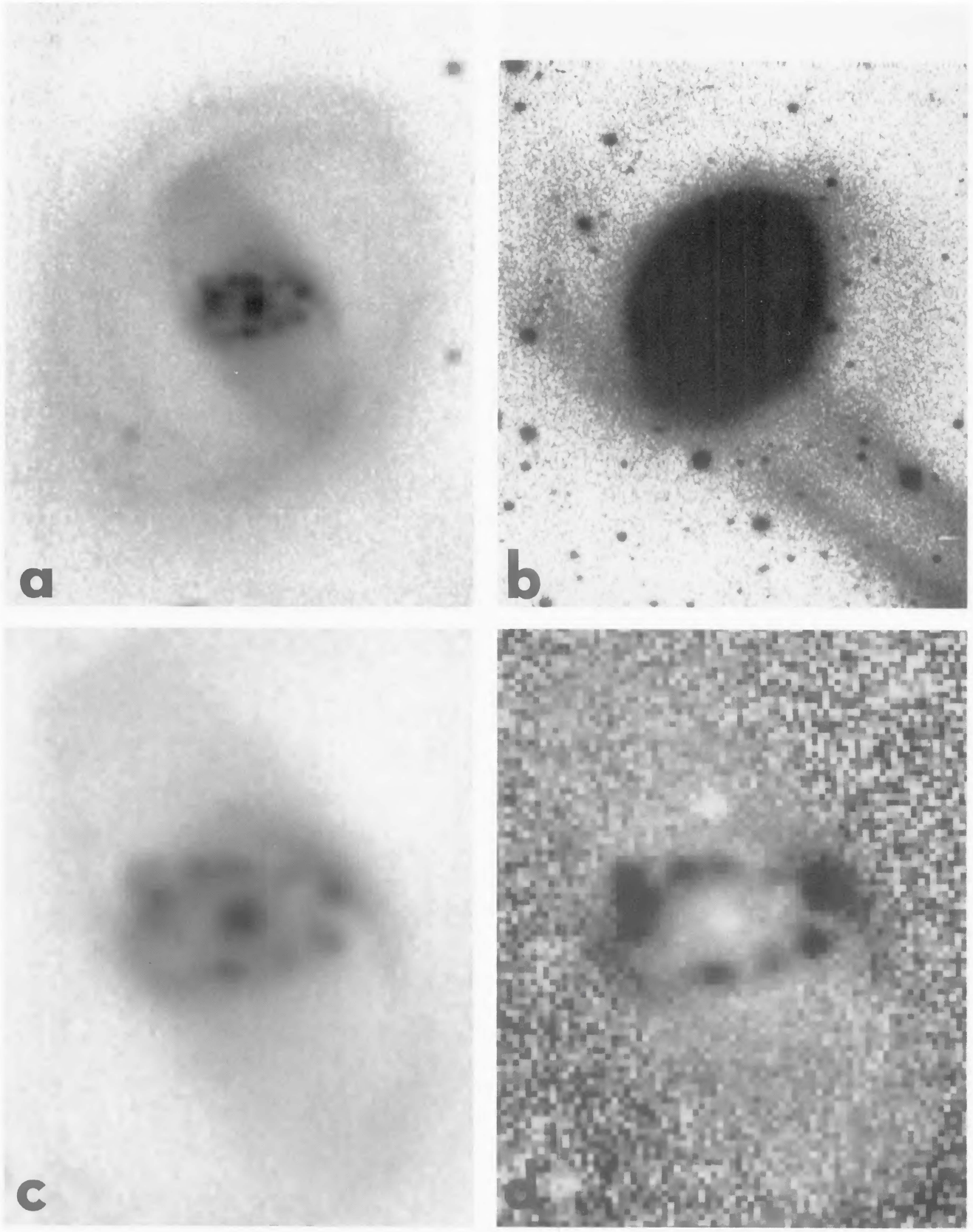

FIG. 11. ESO 565 — 11, an unusual CSRG galaxy with a prominent nuclear ring. Images: (a) *B*, intermediate scale; (b) *B*, small scale to show faint outer structure; (c) *B*, large scale showing nuclear ring; (d) $B - I$, large scale showing nuclear ring.

R. Buta and D. A. Crocker (see page 1718)

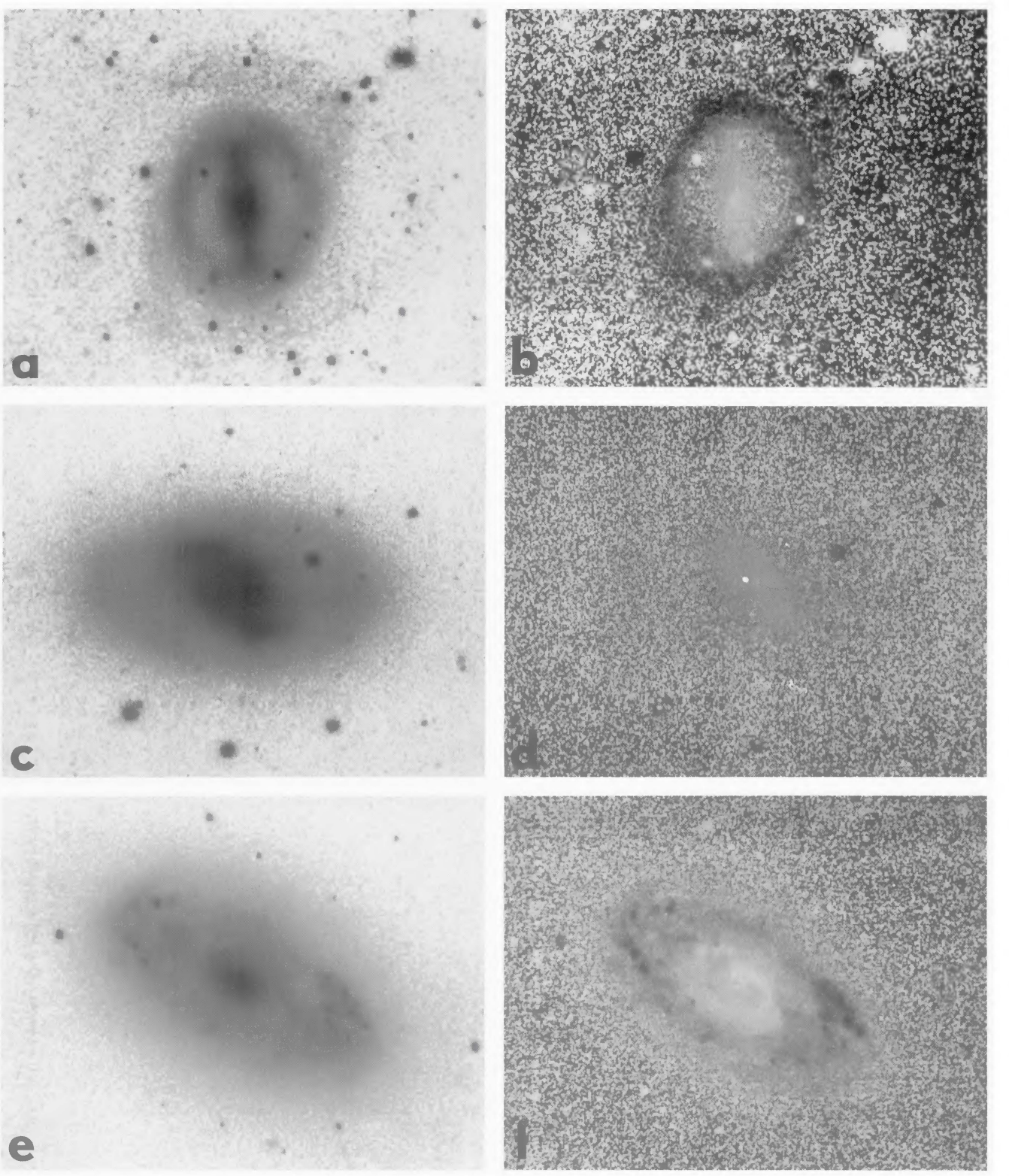

FIG. 12. Three miscellaneous cases from the CSRG (see text): (a) IC 4290 (B); (b) IC 4290 ($B-I$); (c) NGC 2983 (B); (d) NGC 2983 ($B-V$); (e) NGC 5134 (B); (f) NGC 5134 ($B-I$).

R. Buta and D. A. Crocker (see page 1718)

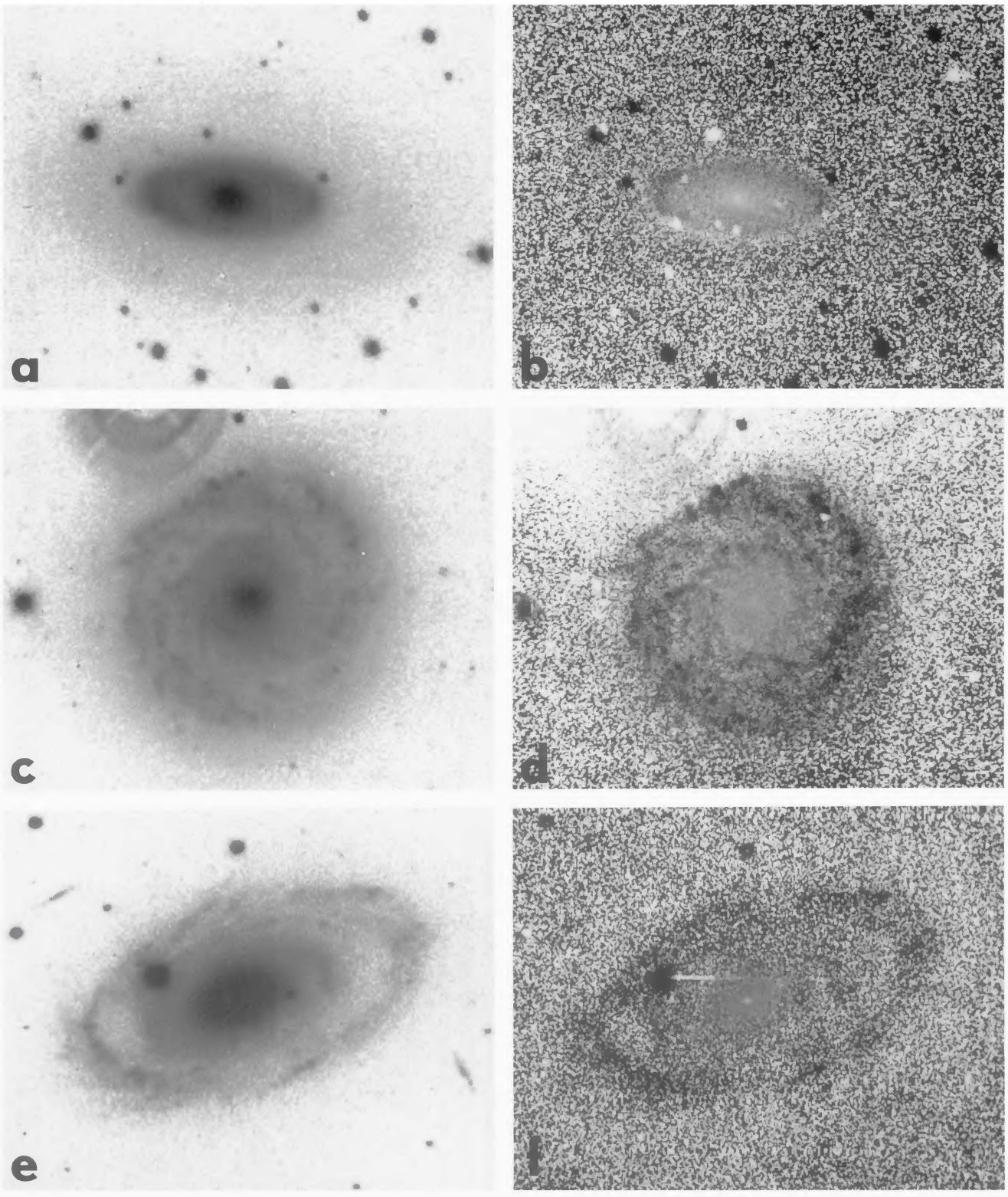

FIG. 13. Examples of rings and pseudorings in three SA galaxies: (a) NGC 4553 (B); NGC 4553 ($B - I$); (c) IC 1993 (B); (d) IC 1993 ($B - I$); (e) ESO 501 − 51 (B); (f) ESO 501 − 51 ($B - I$).

R. Buta and D. A. Crocker (see page 1718)